Resonant enhanced multiphoton ionization studies in atomic oxygen

S. N. Dixit

Lawrence Livermore National Laboratory, University of California, P.O. Box 808, Livermore, California 94550

D. A. Levin

Institute for Defense Analyses, 1801 North Beauregard Street, Alexandria, Virginia 22311

B. V. McKoy

Noyes Laboratory of Chemical Physics, California Institute of Technology, Pasadena, California 91125

(Received 11 December 1987)

In this paper we analyze two-photon-resonant three-photon ionization of atomic oxygen via the $2p^3(^4S^\circ)np\ ^3P_{0,1,2}$ and the $2p^3(^4S^\circ)nf\ ^3F_{2,3,4}$ states. The various atomic parameters required for calculating the resonant enhanced multiphoton ionization (REMPI) probabilities are obtained using quantum-defect theory. The infinite sums over nonresonant states are truncated at a finite number of terms. Our calculated two-photon excitation cross sections agree well with the results of other recent calculations and of experimental measurements. The photoionization cross section is calculated for various electron kinetic energies. The REMPI dynamics is analyzed by solving the density-matrix equations. This framework consistently takes into account the effects of saturation and ac Stark shifts. REMPI probability is seen to be quite sensitive to the initial detuning, the intensity, and the particular resonant state accessed. The photoionization cross sections also imply that due to the rapid falloff of the cross section, two-color REMPI schemes with a lower-frequency ionizing photon would increase the effective REMPI probability.

I. INTRODUCTION

Resonant-enhanced multiphoton ionization (REMPI) is now established as a powerful technique for ultrasensitive detection of atoms and molecules. With its resonance enhancement, REMPI processes usually require lower laser intensities than does a nonresonant multiphoton ionization process. The analysis of REMPI, on the other hand, can be complicated by saturation and laser pulse shape effects and a deconvolution of the observed ion and/or electron signals to extract atomic cross sections is not straightforward.[1] Only at weak power levels is such an extraction convenient.

Atmospheric studies using laser techniques require knowledge of multiphoton ionization probabilities in atomic oxygen. Resonant two-photon absorption has been suggested as a possible scheme for monitoring atomic oxygen concentration.[2] Knowledge of accurate REMPI cross sections are again needed in assessing the feasibility of such schemes. Although there have been calculations of two-photon excitation cross sections in oxygen,[3-6] to our knowledge no published theoretical multiphoton ionization studies exist.

In this paper, we present the results of studies of the two-photon-resonant three-photon ionization of atomic oxygen using quantum-defect theory to calculate the relevant atomic parameters. The REMPI dynamics is analyzed using the density-matrix equations which properly account for the effects of saturation and a.c. Stark shifts. Studies are carried out for (2+1) REMPI via the $2p^3(^4S^\circ)np\ ^3P_{0,1,2}$ for $n = 3-6$ and the $2p^3(^4S^\circ)nf\ ^3F_{2,3,4}$

for $n = 4-7$ states. These states are accessible with available laser sources and are presently under experimental investigation.[7] Our results should therefore be directly comparable with forthcoming experimental data.

The paper is organized as follows. Section II briefly describes the density-matrix framework necessary for analyzing the REMPI dynamics. The equations of motion are written in a general form so that they would be useful in other related REMPI studies. Section III gives the details of the calculations of relevant atomic parameters. General expressions are given for Rabi frequencies, ionization widths, and ac Stark shifts. The angular momentum algebra has been carried out explicitly and the formal expressions of Sec. II are reduced to those containing radial matrix elements and phase shifts as parameters. Results of the quantum-defect calculation of atomic transition matrix elements are presented in Sec. IV. Comparison is made with earlier published results where appropriate. The multiphoton ionization dynamics is then analyzed using these quantities and the results are discussed in Sec. V.

II. REMPI EQUATIONS OF MOTION

In this section we briefly present the derivation of the density-matrix equations for analyzing the dynamics of the two-photon-resonant three-photon (2+1) ionization process. The outer-shell electron configuration of ground-state oxygen is $2p^4(^3P_2)$ with the $^3P_1$ and $^3P_0$ states lying about 159 and 227 cm^{-1} above the ground state. As the separations are well outside the typical laser widths, a particular J_0 level of the $2p^4(^3P)$ configuration

can be chosen as the initial state in the excitation. Based on the available spectroscopic data,[8] the accessible bound excited states are all of the type $2p^3(^4S°)nl \ ^{3,5}L$ with much smaller fine structure splitting than in the ground state. The small fine-structure splitting also implies that intercombination transitions will be weak. Thus here we only consider the triplet states in these REMPI studies. The maximum number of J's for a given triplet configuration will be 3. Although the fine structure in the excited state cannot be resolved, it is still convenient to consider excitations within the $|JM_J\rangle$ basis than in the $|LM_LSM_S\rangle$ basis. One can then readily take advantage of the Wigner-Eckart theorem and related tensorial results. For linearly polarized excitation $\Delta M_J=0$ and hence, transitions originating at a given M_{J_0} of the initial state form an independent channel. It can be easily shown that the maximum number of resonant intermediate states with a given M_J can be three. Thus the ground state, together with the three (at most) resonant states, gives rise to a four-level system coupled to the ionization continuum.

The derivation of the density-matrix equations governing the REMPI dynamics proceeds along the same lines as described in Refs. 9 and 10. The main difference is the generalization to three intermediate resonant states. As this generalization is fairly straightforward, we shall give below only the final form of the differential equations after assuming the rotating wave approximation and adiabatic elimination of the nonresonant intermediate states at the one-photon level and the ionization continuum. The details of this procedure can be found in Refs. 9 and 10.

Denoting by $|0\rangle$, $|1\rangle$, $|2\rangle$, and $|3\rangle$ the states $|2p^4 \ ^3P_{J_0}; J_0M_{J_0}\rangle$, $|2p^3(^4S°)nl \ ^3L_{J_i}; J_iM_{J_i}\rangle$, $i=1,3$ (of course, $M_{J_0}=M_{J_i}$), respectively, the density-matrix equations governing the evolution of the four-level system can be written as follows:

$$\frac{d}{dt}\rho_{00} = -\tfrac{1}{2}i(\Omega_{01}\rho_{10}-\text{c.c.}) - \tfrac{1}{2}i(\Omega_{02}\rho_{20}-\text{c.c.})$$
$$-\tfrac{1}{2}i(\Omega_{03}\rho_{30}-\text{c.c.}) , \qquad (1a)$$

$$\gamma\rho_{11} + \left[\frac{d}{dt}+\Gamma_1\right]\rho_{11}$$
$$= \tfrac{1}{2}i(\Omega_{01}\rho_{10}-\text{c.c.}) + \tfrac{1}{2}i(\Omega_{12}^*\rho_{12}-\text{c.c.})$$
$$+ \tfrac{1}{2}i(\Omega_{13}^*\rho_{13}-\text{c.c.}) , \qquad (1b)$$

$$\gamma\rho_{22} + \left[\frac{d}{dt}+\Gamma_2\right]\rho_{22}$$
$$= \tfrac{1}{2}i(\Omega_{02}\rho_{20}-\text{c.c.}) + \tfrac{1}{2}i(\Omega_{21}^*\rho_{21}-\text{c.c.})$$
$$+ \tfrac{1}{2}i(\Omega_{23}^*\rho_{23}-\text{c.c.}) , \qquad (1c)$$

$$\gamma\rho_{33} + \left[\frac{d}{dt}+\Gamma_3\right]\rho_{33}$$
$$= \tfrac{1}{2}i(\Omega_{03}\rho_{30}-\text{c.c.}) + \tfrac{1}{2}i(\Omega_{31}^*\rho_{31}-\text{c.c.})$$
$$+ \tfrac{1}{2}i(\Omega_{32}^*\rho_{32}-\text{c.c.}) , \qquad (1d)$$

$$\frac{\gamma}{2}\rho_{10} + \left[\frac{d}{dt}-i\Delta_1+\frac{\Gamma_1}{2}\right]\rho_{10}$$
$$= \tfrac{1}{2}i\Omega_{10}(\rho_{11}-\rho_{00}) - \tfrac{1}{2}i\Omega_{12}\rho_{20} - \tfrac{1}{2}i\Omega_{13}\rho_{30}$$
$$+ \tfrac{1}{2}i\Omega_{20}\rho_{12} + \tfrac{1}{2}i\Omega_{30}\rho_{13} , \qquad (1e)$$

$$\frac{\gamma}{2}\rho_{20} + \left[\frac{d}{dt}-i\Delta_2+\frac{\Gamma_2}{2}\right]\rho_{20}$$
$$= \tfrac{1}{2}i\Omega_{20}(\rho_{22}-\rho_{00}) - \tfrac{1}{2}i\Omega_{21}\rho_{10} - \tfrac{1}{2}i\Omega_{23}\rho_{30}$$
$$+ \tfrac{1}{2}i\Omega_{10}\rho_{21} + \tfrac{1}{2}i\Omega_{30}\rho_{23} , \qquad (1f)$$

$$\frac{\gamma}{2}\rho_{30} + \left[\frac{d}{dt}-i\Delta_3+\frac{\Gamma_3}{2}\right]\rho_{30}$$
$$= \tfrac{1}{2}i\Omega_{30}(\rho_{33}-\rho_{00}) - \tfrac{1}{2}i\Omega_{31}\rho_{10} - \tfrac{1}{2}i\Omega_{32}\rho_{20}$$
$$+ \tfrac{1}{2}i\Omega_{10}\rho_{31} + \tfrac{1}{2}i\Omega_{20}\rho_{32} , \qquad (1g)$$

$$\gamma\rho_{12} + \left[\frac{d}{dt}+i(\omega_{12}+S_{12})+\tfrac{1}{2}(\Gamma_1+\Gamma_2)\right]\rho_{12}$$
$$= -\tfrac{1}{2}i\Omega_{10}\rho_{02} + \tfrac{1}{2}i\Omega_{02}\rho_{10}$$
$$+ \tfrac{1}{2}i(\rho_{11}\Omega_{12}^*+\rho_{13}\Omega_{32}^*-\Omega_{12}\rho_{22}-\Omega_{13}\rho_{32}) , \qquad (1h)$$

$$\gamma\rho_{23} + \left[\frac{d}{dt}+i(\omega_{23}+S_{23})+\tfrac{1}{2}(\Gamma_2+\Gamma_3)\right]\rho_{23}$$
$$= -\tfrac{1}{2}i\Omega_{20}\rho_{03} + \tfrac{1}{2}i\Omega_{03}\rho_{20}$$
$$+ \tfrac{1}{2}i(\rho_{21}\Omega_{13}^*+\rho_{22}\Omega_{23}^*-\Omega_{21}\rho_{13}-\Omega_{23}\rho_{33}) , \qquad (1i)$$

$$\gamma\rho_{31} + \left[\frac{d}{dt}+i(\omega_{31}+S_{31})+\tfrac{1}{2}(\Gamma_3+\Gamma_1)\right]\rho_{31}$$
$$= -\tfrac{1}{2}i\Omega_{30}\rho_{01} + \tfrac{1}{2}i\Omega_{01}\rho_{30}$$
$$+ \tfrac{1}{2}i(\rho_{32}\Omega_{21}^*+\rho_{33}\Omega_{31}^*-\Omega_{31}\rho_{11}-\Omega_{32}\rho_{21}) . \qquad (1j)$$

In these equations, Ω_{01}, Ω_{02}, and Ω_{03} denote the two-photon Rabi frequencies from the ground state to the resonant state and Γ_1, Γ_2, and Γ_3 the ionization widths out of the resonant states. Δ_1, Δ_2, and Δ_3 are the detunings of the two photons from the ac Stark shifted energy difference between the ground and resonant states; i.e.,

$$\Delta_1 = 2\omega-(\omega_1-\omega_0)-(S_1-S_0) . \qquad (1k)$$

S_i denotes the a.c. Stark shift of state $|i\rangle$, $\omega_{ij}=\omega_i-\omega_j$, and $S_{ij}=S_i-S_j$. γ is the spontaneous decay width out of the resonant states and is assumed to be the same for all fine-structure multiplets. Finally, Ω_{12}, Ω_{23}, and Ω_{31} are complex and describe the interference between the various ionization channels ($\Omega_{ji}=\Omega_{ij}$). For simplicity, we ignore the effects of laser linewidth and lineshape. Whenever the number of resonant states is less than three, a reduced set of equations from the above can be obtained. Equation (1) describes accurately the dynamics of the four-level system taking into account the effects of saturation and ac Stark shifts. The detailed expressions for these various parameters are given in Table I. Finally, it

TABLE I. REMPI Dynamics parameters. $\Omega_{ij} = \Omega_{ji}$, I is the intensity in W/cm^2, $\hbar\omega$ is the photon energy in joules, α is the fine-structure constant, $\hbar\omega_j$ are the level energies in joules, and matrix elements are (for this table only) in cm.

$$\Omega_{k0} = 4\pi\alpha I \sum_i \frac{\langle k \mid \mathbf{r}\cdot\boldsymbol{\varepsilon} \mid i \rangle\langle i \mid \mathbf{r}\cdot\boldsymbol{\varepsilon} \mid 0 \rangle}{\hbar\omega_0 - \hbar\omega_k + \hbar\omega}, \quad k = 1,2,3$$

$$S_k - \tfrac{1}{2}i\Gamma_k = 2\pi\alpha I \left[\sum_p \frac{\langle k \mid \mathbf{r}\cdot\boldsymbol{\varepsilon} \mid p \rangle\langle p \mid \mathbf{r}\cdot\boldsymbol{\varepsilon} \mid k \rangle}{\hbar\omega_k - \hbar\omega_p - \hbar\omega} + \sum_q \frac{\langle k \mid \mathbf{r}\cdot\boldsymbol{\varepsilon} \mid q \rangle\langle q \mid \mathbf{r}\cdot\boldsymbol{\varepsilon} \mid k \rangle}{\hbar\omega_k - \hbar\omega_q + \hbar\omega} \right], \quad k = 0,1,2,3$$

$$\Omega_{ij} = \Omega'_{ij} - i\Omega''_{ij} = 4\pi\alpha I \left[\sum_p \frac{\langle i \mid \mathbf{r}\cdot\boldsymbol{\varepsilon} \mid p \rangle\langle p \mid \mathbf{r}\cdot\boldsymbol{\varepsilon} \mid j \rangle}{\hbar\omega_i - \hbar\omega_p - \hbar\omega} + \sum_q \frac{\langle i \mid \mathbf{r}\cdot\boldsymbol{\varepsilon} \mid q \rangle\langle q \mid \mathbf{r}\cdot\boldsymbol{\varepsilon} \mid j \rangle}{\hbar\omega_i - \hbar\omega_q + \hbar\omega} \right], \quad i,j = 1,2,3 \text{ and } i \neq j$$

should be noted that had we described the resonant intermediate state in the $\mid LM_L SM_S \rangle$ representation, one would still have more than one intermediate state since a given $\mid J_0 M_{J_0} \rangle$ state would connect to all states $\mid LM_L SM_S \rangle$ satisfying the condition $M_{J_0} = M_L + M_S$.

III. CALCULATION OF ATOMIC PARAMETERS FOR OXYGEN

A. Simplification of expressions

In this section we briefly describe the calculations of the parameters needed for the determination of the $(2+1)$ REMPI cross section. Except in the ground state, we shall only be interested in the states having a $^4S^\circ$ core. When spin-orbit coupling effects are neglected, it can be shown that terms of the form,

$$\langle 2p^3(^2D)ns(^3D) \mid \mathbf{r}\cdot\boldsymbol{\varepsilon} \mid 2p^3(^4S)np(^3P) \rangle ,$$

are identically zero. The single-photon nonresonant intermediate states contributing to the two-photon Rabi

frequencies will be of the type $2p^3(^4S^\circ)n$'s and $2p^3(^4S^\circ)n'd$ for excitation to the $2p^3\,np$ levels and of the type $2p^3(^4S^\circ)n'd$ for two-photon excitations to $2p^3\,nf$ states. Similarly, the s and d partial waves contribute to the photoionization out of $2p^3\,np$ levels while d and g partial waves contribute to the photoionization widths of $2p^3\,nf$ levels. The bound-bound transition matrix elements can then be calculated using the standard techniques of Racah algebra and fractional parentage.[11] The results are given in Table II. It should be noted that the parameters $A(0)$ and $A(1)$ defined by Saxon and Eichler[5] are related to R_s and R_d via

$$A(0) = -(\tfrac{4}{3})^{1/2}(R_s/3 + \tfrac{4}{15}R_d) , \tag{2a}$$

$$A(1) = \tfrac{1}{5}[-(\tfrac{4}{3})^{1/2}]R_d . \tag{2b}$$

The casting of the formula into R_s and R_d exemplifies the contributions of the ns and nd intermediate states to the two-photon transition.

Similarly, the two-photon excitation cross section for the $J_0 \rightarrow J_i$ transition is given by (in units of cm^4)

$$\sigma_0^{(2)} = \frac{8\pi^3\alpha^2 a_0^4 (\hbar\omega)^2}{2J_0 + 1} \sum_{M_{J_0}, M_{J_i}} \left| \sum_{J', M'} \frac{\langle J_i M_{J_i} \mid \mathbf{r}\cdot\boldsymbol{\varepsilon} \mid J'M' \rangle\langle J'M' \mid \mathbf{r}\cdot\boldsymbol{\varepsilon} \mid J_0 M_{J_0} \rangle}{\hbar\omega_{J_0} - \hbar\omega_{J'} + \hbar\omega} \right|^2 \tag{3a}$$

$$= \frac{\pi}{2} \left[\frac{\hbar\omega}{I} \right]^2 \frac{1}{2J_0 + 1} \sum_{M_{J_0}, M_{J_i}} \left| \Omega_{J_0 M_{J_0} \rightarrow J_i M_{J_i}} \right|^2 , \tag{3b}$$

where the quantity in the summation in (3a) is in atomic units. Expressions used by earlier authors[3-6] can be reproduced from this equation.

For the calculation of bound-free matrix elements, the energy normalized photoelectron continuum wave function as given by Eq. (6) of Ref. 9 is combined with the $2p^3(^4S^\circ)$ core wave function and the matrix elements computed using the Racah algebra.[11] For the purpose of this paper, we will be interested in total, spin-unresolved, angle integrated ionization rates. The phase-shift dependence therefore drops out. The resulting expressions are summarized in Table III. The expressions for ac Stark shifts are similar except for the prefactor being $2\pi\alpha I$ and R_S and R_d denoting the summations over the discrete and continuum states. The expressions for the ground-state a.c. Stark shifts are also given in Table III.

Finally, the calculation of the interference terms Ω_{12}, Ω_{23}, and Ω_{31} is again similar to the calculation of the shift and width parameters, the only difference being that the interference terms involve two different resonant states connecting with the continuum as shown in Table I. Nonzero parameters are given in Table IV. The real part is obtained by dividing the imaginary part by π and regarding $\tilde{R}_s$ and $\tilde{R}_d$ as summations over bound and continuum states.

B. Atomic wave functions

The ground-state wave function is calculated within the single configuration Hartree-Fock approximation using the numerical codes of Froese Fischer.[12] For the

TABLE II. Two-photon-resonant, three-photon-ionization schemes for atomic oxygen.

$$A = 4\pi \alpha I a_0^3/e^2; \quad R_s = \sum_{n'} \frac{\langle np \mid r \mid n's \rangle \langle n's \mid r \mid 2p \rangle}{\hbar\omega_{J_0} - \hbar\omega_J + \hbar\omega}, \quad R_d = \sum_{n'} \frac{\langle np \mid r \mid n'd \rangle \langle n'd \mid r \mid 2p \rangle}{\hbar\omega_{J_0} - \hbar\omega_J + \hbar\omega}$$

for $p \to \to nf$ excitation, $R_d = \sum_{n'} \frac{\langle nf \mid r \mid n'd \rangle \langle n'd \mid r \mid 2p \rangle}{\hbar\omega_{J_0} - \hbar\omega_J + \hbar\omega}$ in a.u.,

$$\Omega_{J_0 M_{J_0} \to J M_J} = Aa(bR_s + cR_d), \quad \Omega_{J_0 M_{J_0} \to J M_J} = (-1)^{J-J_0} \Omega_{J_0 M_{J_0} \to J - M_J},$$

Initial state		Final state $2p^4 \to \to 2p^3 np$ transitions				
J_0	M_{J_0}	J_i	M_{J_i}	a	b	c
2	0	0	0	$\frac{2}{9}\left[\frac{2}{3}\right]^{1/2}$	1	$\frac{1}{5}$
2	1	1	1	$\frac{1}{3\sqrt{3}}$	1	$\frac{1}{5}$
2	1	1	0	0	0	0
2	2	2	2	$-\frac{2}{5\sqrt{3}}$	0	1
2	1	2	1	$-\frac{1}{3\sqrt{3}}$	1	$\frac{7}{5}$
2	0	2	0	$-\frac{2}{9\sqrt{3}}$	2	$\frac{11}{5}$
1	0	0	0	0	0	0
1	1	1	1	$-\frac{1}{3\sqrt{3}}$	1	$\frac{7}{5}$
1	0	1	0	$-\frac{2}{5\sqrt{3}}$	0	1
1	0	2	0	0	0	0
1	1	2	1	$\frac{1}{3\sqrt{3}}$	1	$\frac{1}{5}$
0	0	0	0	$-\frac{2}{9\sqrt{3}}$	1	2
0	0	1	0	0	0	0
0	0	2	0	$\frac{2}{9}\left[\frac{2}{3}\right]^{1/2}$	1	$\frac{1}{5}$

$2p^4 \to \to 2p^3 nf$ transitions; $b = 0$, $c = 1$ in all cases

J_0	M_{J_0}	J	M_J	a
0	0	2	0	$-\frac{4}{15}$
1	0	2	0	0
1	0	3	0	$\frac{4}{5}\left[\frac{2}{21}\right]^{1/2}$
2	0	2	0	$\frac{4\sqrt{2}}{105}$
2	0	3	0	0
2	0	4	0	$-\frac{4\sqrt{6}}{35}$
1	1	2	1	$\frac{2\sqrt{2}}{15}$
1	1	3	1	$-\frac{8}{15\sqrt{7}}$
2	1	2	1	$\frac{2\sqrt{2}}{105}$
2	1	3	1	$\frac{4}{15\sqrt{7}}$
2	1	4	1	$-\frac{4\sqrt{5}}{35}$

TABLE II. (Continued).

$2p^4 \to \to 2p^3 nf$ transitions; $b=0$, $c=1$ in all cases				
J_0	M_{J_0}	J	M_J	a
2	2	2	2	$-\dfrac{4\sqrt{2}}{105}$
2	2	3	2	$\dfrac{2\sqrt{2}}{3\sqrt{35}}$
2	2	4	2	$-\dfrac{2}{7}\left[\dfrac{2}{5}\right]^{1/2}$

TABLE III. Ionization widths. $\tilde{R}_s$, $\tilde{R}_d$, and $\tilde{R}_g$ are in a.u.

J	M_J	a	b
		Out of $2p^3\,np$ levels $\Gamma_{JM_J} = 4\pi^2\alpha I a_0^2(a\tilde{R}_s^2 + b\tilde{R}_d^2)$	
0	0	$\frac{1}{9}$	$\frac{2}{9}$
1	1	$\frac{1}{6}$	$\frac{7}{30}$
1	0	0	$\frac{1}{5}$
2	2	0	$\frac{1}{5}$
2	1	$\frac{1}{6}$	$\frac{7}{30}$
2	0	$\frac{2}{9}$	$\frac{11}{45}$
		Out of $2p^3\,nf$ levels (only $M_J \le 2$ are needed) $\Gamma_{JM_J} = 4\pi^2\alpha I a_0^2(a\tilde{R}_d^2 + b\tilde{R}_g^2)$	
2	2	$\frac{11}{245}$	$\frac{20}{147}$
2	1	$\frac{47}{245}$	$\frac{32}{147}$
2	0	$\frac{59}{245}$	$\frac{12}{49}$
3	2	$\frac{1}{7}$	$\frac{4}{21}$
3	1	$\frac{29}{140}$	$\frac{19}{84}$
3	0	$\frac{8}{35}$	$\frac{5}{21}$
4	2	$\frac{9}{49}$	$\frac{94}{441}$
4	1	$\frac{45}{196}$	$\frac{421}{36\times49}$
4	0	$\frac{12}{49}$	$\frac{109}{9\times49}$
		Ground-state shifts $S_{J_0 M_{J_0}} = 2\pi\alpha I a_0^2(a\tilde{R}_s^2 + b\tilde{R}_d^2)$	
0	0	$\frac{4}{27}$	$\frac{8}{27}$
1	1	$\frac{2}{9}$	$\frac{14}{45}$
1	0	0	$\frac{4}{15}$
2	2	0	$\frac{4}{15}$
2	1	$\frac{2}{9}$	$\frac{14}{45}$
2	0	$\frac{8}{27}$	$\frac{44}{135}$

excited-state and the continuum wave functions we used the single-channel quantum-defect theory. This should be quite accurate, as the position of the excited levels indicates a nearly constant quantum defect for each series: $\mu_s \approx 1.15$, $\mu_p \approx 0.7$, and $\mu_d \approx 0.02$. All other series are treated as purely hydrogenic with zero quantum defects. The summations over the intermediate states are performed by truncating them to a certain value of n. We have chosen n about 20 for both s and d channels. The accuracy of this truncation depends on the level of excitation. We have also used the quantum-defect theory Green's function to check the accuracy of our truncation.

TABLE IV. Nonzero interference terms. $\tilde{R}_s$, $\tilde{R}_d$, and $\tilde{R}_g$ are in a.u.

$$2p^4 \to \to 2p^3\,np\ (^3P_{0,1,2})$$
$$1{:}J=0,\ 2{:}J=1,\ 3{:}J=2,\ \Omega_{ij}=\Omega'_{ij}-i\Omega''_{ij};\Omega_{ji}=\Omega_{ij}$$

$$M_J=1{:}\Omega''_{23}=4\pi^2\alpha I a_0^2\left(-\tfrac{1}{6}\tilde{R}_s^2-\tfrac{1}{30}\tilde{R}_d^2\right)$$

$$M_J=0{:}\Omega''_{31}=4\pi^2\alpha I a_0^2\left[-\frac{\sqrt{2}}{9}\tilde{R}_s^2-\frac{\sqrt{2}}{45}\tilde{R}_d^2\right]$$

$$2p^4 \to \to 2p^3\,nf(^3F_{2,3,4})$$
$$1{:}J=2,\ 2{:}J=3,\ 3{:}J=4$$

$$M_J=0{:}\Omega''_{13}=4\pi^2\alpha I a_0^2\left[-\frac{2\sqrt{3}}{5\times49}\tilde{R}_d^2-\frac{2\sqrt{3}}{49\times9}\tilde{R}_g^2\right]$$

$$M_J=1{:}\Omega''_{12}=4\pi^2\alpha I a_0^2\left[-\frac{6}{35\sqrt{14}}\tilde{R}_d^2-\frac{2}{21\sqrt{14}}\tilde{R}_g^2\right]$$

$$\Omega''_{23}=4\pi^2\alpha I a_0^2\left[-\frac{5}{28\sqrt{35}}\tilde{R}_d^2-\frac{25}{9\times28\sqrt{35}}\tilde{R}_g^2\right]$$

$$\Omega''_{31}=4\pi^2\alpha I a_0^2\left[-\frac{2}{49\sqrt{10}}\tilde{R}_d^2-\frac{\sqrt{10}}{9\times49}\tilde{R}_g^2\right]$$

$$M_J=2{:}\Omega''_{12}=4\pi^2\alpha I a_0^2\left[-\frac{3}{7\sqrt{35}}\tilde{R}_d^2-\frac{5}{21\sqrt{35}}\tilde{R}_g^2\right]$$

$$\Omega''_{23}=4\pi^2\alpha I a_0^2\left[-\frac{1}{7\sqrt{7}}\tilde{R}_d^2-\frac{5}{63\sqrt{7}}\tilde{R}_g^2\right]$$

$$\Omega''_{31}=4\pi^2\alpha I a_0^2\left[-\frac{1}{49\sqrt{5}}\tilde{R}_d^2-\frac{5}{49\times9\sqrt{5}}\tilde{R}_g^2\right]$$

For the s channel, the truncated $3p$ excitation amplitude is within 5% of the Green's function result while the difference increases to 40% for the $6p$. The accuracy of the Green's function result in the d channel is difficult to assess as the quantum-defect parameter $(\mu \sim 0.022)$ is extremely small and hence is sensitive to the accuracy of the energy level spacings. Nevertheless, the truncated summation two-photon excitation cross sections are in good agreement with the results of Saxon and Eichler[5] and others.[3,4,6] For example, we obtain a value of

11.97×10^{-36} cm^4 compared with 13.19×10^{-36} cm^4 of Ref. 5 for the two-photon excitation to the $2p^3 3p$ state. Similarly, the calculated photoionization cross section of 4.15×10^{-19} cm^2 out of the $3p$ level agrees well with the experimentally deduced value of $(5.3 \pm 2) \times 10^{-19}$ cm^2 by Bamford et al.[7] Thus we believe that our calculated parameters should be fairly accurate. The summations over the off-resonant states in the expressions for the a.c. Stark shifts are also truncated to $n = 20$. The various parameters for the $(2+1)$ REMPI via the $2p^3({}^4S°)np\ {}^3P$ states

TABLE V. Parameters for $(2+1)$ REMPI via the $2p^3 np$ levels (all parameters are in sec^{-1}/W cm^{-2} and are written as aI, where I is the laser intensity in W/cm^2).

J_0	M_{J_0}	J_i	$n = 3$	$n = 4$	$n = 5$	$n = 6$
				Rabi frequencies		
0	0	0	−2.53	−0.742	−0.515	−0.298
0	0	2	1.86	0.828	−0.579	0.456
1	0	1	−1.21	−0.156	−0.106	0.0241
2	0	0	1.86	0.828	0.579	0.456
2	0	2	−3.84	−1.33	−0.924	−0.620
1	1	1	−3.18	−1.03	−0.719	−0.459
1	1	2	1.97	0.879	0.614	0.483
2	1	1	1.97	0.879	0.614	0.483
2	1	2	−3.18	−1.03	−0.719	−0.459
2	2	2	−1.21	−0.156	−0.106	0.0241

J_i	M_{J_i}		$n = 3$	$n = 4$	$n = 5$	$n = 6$
				Ionization widths		
0	0		0.471	0.169	0.0755	0.0393
1	0		0.128	0.073	0.0344	0.0180
2	0		0.813	0.267	0.117	0.0606
1	1		0.642	0.218	0.0961	0.049
2	1		0.642	0.218	0.0961	0.049
2	2		0.128	0.073	0.0344	0.018

J_0	M_{J_0}		$n = 3$	$n = 4$	$n = 5$	$n = 6$
				ac Stark shifts—ground state		
0	0		−0.233	−0.261	−0.274	−0.282
1	0		−0.055	−0.0588	−0.060	−0.061
2	0		−0.410	−0.463	−0.488	−0.503
1	1		−0.321	−0.362	−0.381	−0.392
2	1		−0.321	−0.362	−0.381	−0.392
2	2		−0.549	−0.588	−0.060	−0.061

J_i	M_{J_i}		$n = 3$	$n = 4$	$n = 5$	$n = 6$
				ac Stark shifts—excited state		
0	0		6.51	5.32	4.92	4.70
1	0		6.78	5.48	5.07	4.86
2	0		6.24	5.15	4.76	4.55
1	1		6.37	5.23	4.84	4.63
2	1		6.37	5.23	4.84	4.63
2	2		6.78	5.48	5.07	4.86

	$n = 3$	$n = 4$	$n = 5$	$n = 6$
		Interference terms		
$\Omega'_{31}(M_{J_i} = 0)$	0.764	0.474	0.4395	0.436
$\Omega''_{31}\ (M_{J_i} = 0)$	−0.484	−0.137	−0.0582	−0.0300
$\Omega'_{23}\ (M_{J_i} = 1)$	0.810	0.503	0.4662	0.462
$\Omega''_{23}\ (M_{J_i} = 1)$	−0.513	−0.145	−0.06169	−0.03193

TABLE VI. Parameters for $(2+1)$ REMPI via the $2p^3 nf$ levels.

J_0	M_{J_0}	J_i	$n=4$	$n=5$	$n=6$	$n=7$
				Rabi frequencies		
2	2	4	0.367	0.176	0.0983	0.0457
2	2	3	−0.324	−0.155	−0.0867	−0.0403
2	2	2	0.109	0.0526	0.0293	0.0136
2	1	4	0.519	0.249	0.139	0.0647
2	1	3	−0.205	−0.0983	−0.0548	−0.2055
2	1	2	−0.548	−0.0263	−0.0147	−0.00682
2	0	4	0.569	0.273	0.152	0.0708
2	0	2	−0.109	−0.0526	−0.0293	−0.0136
1	1	2	−0.383	−0.184	−0.1026	−0.0477
1	0	3	−0.502	−0.241	−0.134	−0.0625
1	1	3	0.409	0.197	0.109	0.0510
0	0	2	0.542	0.260	0.145	0.0675

J_i	M_{J_i}	$n=4$	$n=5$	$n=6$	$n=7$
			Ionization widths		
2	4	0.311×10^{-2}	0.204×10^{-2}	0.129×10^{-2}	0.844×10^{-3}
2	3	0.278×10^{-2}	0.182×10^{-2}	0.115×10^{-2}	0.753×10^{-3}
2	2	0.196×10^{-2}	0.128×10^{-2}	0.810×10^{-3}	0.535×10^{-3}
1	4	0.349×10^{-2}	0.229×10^{-2}	0.145×10^{-2}	0.947×10^{-3}
1	3	0.331×10^{-2}	0.217×10^{-2}	0.137×10^{-2}	0.897×10^{-3}
1	2	0.318×10^{-2}	0.209×10^{-2}	0.132×10^{-2}	0.863×10^{-3}
0	4	0.362×10^{-2}	0.237×10^{-2}	0.149×10^{-2}	0.981×10^{-3}
0	3	0.349×10^{-2}	0.229×10^{-2}	0.144×10^{-2}	0.944×10^{-3}
0	2	0.359×10^{-2}	0.235×10^{-2}	0.48×10^{-2}	0.972×10^{-3}

J_0	M_{J_0}	$n=4$	$n=5$	$n=6$	$n=7$
			ac Stark shifts—ground state		
2	2	−0.0599	−0.0609	−0.0616	−0.0619
2	1	−0.377	−0.389	−0.397	−0.402
2	0	−0.482	−0.4991	−0.509	−0.515
1	1	−0.377	−0.389	−0.397	−0.402
1	0	−0.0599	−0.0609	−0.0616	−0.0619
0	0	−0.2711	−0.280	−0.285	−0.289

J_i	M_{J_i}	$n=4$	$n=5$	$n=6$	$n=7$
			ac Stark shifts—excited state		
2	4	4.68	4.08	3.69	3.41
2	3	4.79	4.25	3.89	3.65
2	2	5.07	4.64	4.39	4.22
1	4	4.55	3.89	3.47	3.14
1	3	4.61	3.99	3.56	3.27
1	2	4.66	4.05	3.65	3.36
0	4	4.51	3.84	3.39	3.05
0	3	4.55	3.90	3.47	3.14
0	2	4.52	3.85	3.41	3.07

	$n=4$	$n=5$	$n=6$	$n=7$
		Interference terms $M_{J_i}=0$		
Ω'_{13}	3.94×10^{-2}	5.65×10^{-2}	7.06×10^{-2}	8.298×10^{-2}
Ω''_{13}	-1.17×10^{-4}	-7.71×10^{-5}	-4.87×10^{-5}	-3.148×10^{-5}

TABLE VI. (Continued).

	$n=4$	$n=5$	$n=6$	$n=7$
		Interference terms $M_{J_i}=1$		
Ω'_{12}	0.128	0.183	0.229	0.269
Ω''_{12}	-3.80×10^{-4}	-2.49×10^{-4}	-1.57×10^{-4}	-1.02×10^{-4}
Ω'_{23}	8.43×10^{-2}	0.120	0.151	0.177
Ω''_{23}	-2.51×10^{-4}	-1.65×10^{-4}	-1.04×10^{-4}	-6.72×10^{-5}
Ω'_{13}	3.60×10^{-2}	5.16×10^{-2}	6.45×10^{-2}	7.57×10^{-2}
Ω''_{13}	-1.071×10^{-4}	-7.04×10^{-5}	-4.44×10^{-5}	-2.87×10^{-5}
	$n=4$	$n=5$	$n=6$	$n=7$
		Interference terms $M_{J_i}=2$		
Ω'_{12}	0.202	0.289	0.362	0.425
Ω''_{12}	-6.02×10^{-5}	-3.95×10^{-5}	-2.49×10^{-5}	-1.61×10^{-4}
Ω'_{23}	0.151	0.216	0.269	0.317
Ω''_{23}	-4.48×10^{-4}	-2.94×10^{-4}	-1.86×10^{-4}	-1.20×10^{-4}
Ω'_{13}	2.55×10^{-2}	3.65×10^{-2}	4.56×10^{-2}	5.35×10^{-2}
Ω''_{13}	-7.58×10^{-5}	-4.98×10^{-5}	-3.14×10^{-5}	-2.03×10^{-5}

for $n=3-6$ and via the $2p^3(^4S°)nf\,^3F$, $n=4-7$ are shown in Tables V and VI. The photon frequency for each case is chosen to be equal to half the energy difference between the ground and resonant state.

IV. REMPI DYNAMICS

Equation (1), together with the parameters in Tables V and VI, are sufficient to analyze the dynamics of the multiphoton ionization process. The ionization probability is calculated for each $|J_0 M_{J_0}\rangle$ channel by solving the density-matrix equations and is subsequently averaged over the initial M_{J_0} levels. The effects of saturation and a.c. Stark shifts are automatically taken into account in the solution. For the purpose of the discussion in this paper, we shall assume a spatially uniform pulse turned on to its peak intensity value at $t=0$ and turned off at $t=T$. The results presented here are for $T=5$ nsec. A typical plot of the ionization probability versus laser intensity is shown in Fig. 1 for the $2p^4(^3P_2)\rightarrow\rightarrow 2p^3(^4S°)3p\,^3P_{0,1,2}$ excitation. For low intensities, one observes a cubic dependence on intensity characteristic of a three-photon process. The ionization probability saturates at high intensities. However, for positive detunings (two-photon energy larger than the level spacing), the effect of a.c. Stark shifts is quite evident. The levels, initially off-resonant, are tuned into and then out of resonance with increasing intensity. This dynamic tuning in and out of resonance appears as a peak in the ionization probability. The sharpness of the peak is a consequence of the low values of ionization cross sections. We find that the photoionization cross section increases rather sharply with decreasing photoelectron kinetic energy. Thus, a two-color multiphoton ionization scheme with a much shorter ionization photon energy would enhance the cross section. The results for the other intermediate states are very similar to those for the $3p$ intermediate level but with intensities scaled upwards due to the smaller atomic parameters. Figure 2 shows the probability of ionization as a function of detuning for different laser intensities. The figure shows that at 10 GW/cm², the shifting of the

resonance frequency to positive detunings increases for larger intensities. The figure also shows that to obtain 50% ionization within ±1 cm^{-1} tunability, laser intensities on the order of 10 GW/cm² will be necessary.

Finally, it should be noted that we have neglected the effects of laser and Doppler broadening and the effects of the spatial-temporal profile of the laser pulse. The emphasis was more on the calculation of atomic parameters
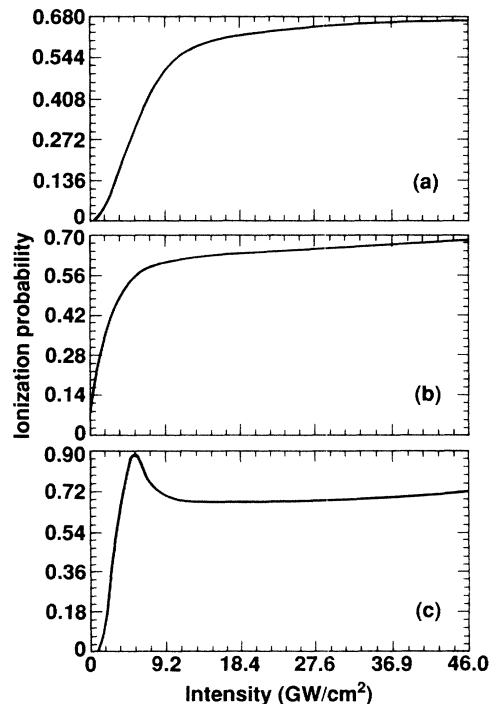
FIG. 1. Probability of ionization as a function of laser intensity and resonance detuning through the $3p$ intermediate state: (a) detuning$=-0.2$ cm^{-1}, (b) detuning$=0.0$ cm^{-1}, and (c) detuning $=0.2$ cm^{-1}.
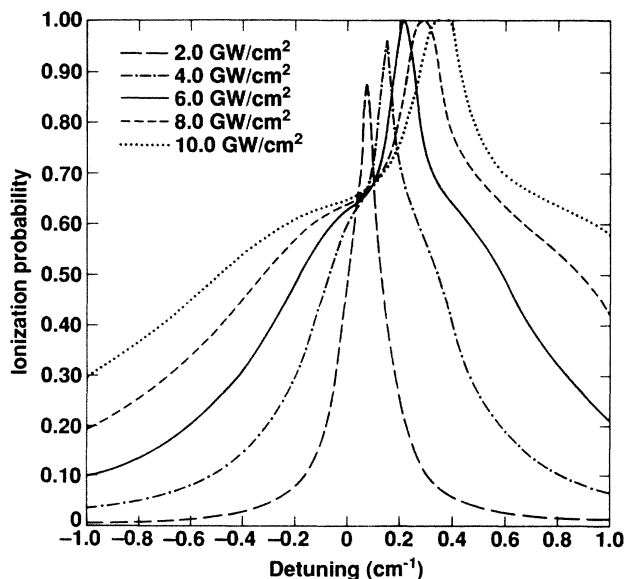
FIG. 2. Probability of ionization as a function of detuning for different laser intensities through the $3p$ intermediate state and a pulse duration of 10 rs.

than on such geometrical effects. The effects of Doppler-broadened laser line shape and its spatial-temporal variations are generally understood. It could be expected that the broadening mechanisms will increase the intensity requirements. Averaging over the spatial variation of the laser intensity would wash out features such as the sharp a.c. Stark shifted peak and lead to shoulders in the averaged ionization probability. Likewise, the volume effect

will cause the averaged probability to continue increasing beyond the saturation intensity.

V. SUMMARY AND CONCLUSIONS

We have presented detailed *ab initio* calculations for two-photon-resonant three-photon ionization of atomic oxygen via the $2p^3 np$ and $2p^3 nf$ levels. Our calculations indicate that transitions via the $3p$ level lead to the most efficient ionization. Even this scheme requires a few GW/cm^2 for a 5 nsec pulse to achieve about 50% ionization. At these intensities the ac Stark shifts are shown to be significant. A two-color scheme ionizing close to the threshold is expected to increase the ionization rate.

Our calculations have neglected the effect of autoionizing states converging to the $2p^3{}^2D$ and ^2P limits. The photon energies are such that three photons excite the atom into the conjested autoionizing region. A description of the final state taking into account the interaction between the discrete states and the continuum is desirable. Such an analysis, using the multichannel quantum-defect theory is currently underway and the results will be published elsewhere.

[1]For aspects of resonant multiphoton ionization, see, *Multiphoton Ionization of Atoms*, edited by S. L. Chin and P. Lambropoulos (Academic, New York, 1976).

[2]T. J. McIlrath, R. Hudson, A. Aiken, and T. D. Wilkerson, App. Opt. **18**, 316 (1979).

[3]K. Omidvar, Phys. Rev. A **22**, 1576 (1980); **30**, 2805 (1984).

[4]M. S. Pindzola, Phys. Rev. A **17**, 1201 (1978).

[5]R. P. Saxon and J. Eichler, Phys. Rev. A **34**, 199 (1986).

[6]E. J. McGuire, Sandia National Laboratory Report No. SAND-85-2374 (unpublished).

[7]D. J. Bamford, L. E. Jusinski, and W. K. Bischel, Phys. Rev. A **34**, 185 (1986).

[8]C. E. Moore, *Atomic Energy Levels*, Natl. Bur. Stand. (U.S.) Circ. No. 467 (U.S. GPO, Washington, DC, 1949), Vol. 1.

[9]S. N. Dixit and P. Lambropoulos, Phys. Rev. A **27**, 861 (1983).

[10]S. N. Dixit, P. Lambropoulos, and P. Zoller, Phys. Rev. A **24**, 318 (1981).

[11]I. Sobelman, *Introduction to the Theory of Atomic Spectra* (Pergamon, New York, 1972).

[12]C. Froese Fischer, Comput. Phys. Commun. **14**, 145 (1978).